

**Key words:** *fatigue crack growth, fatigue tests, overloads, crack closure*

MALGORZATA SKORUPA<sup>\*)</sup>, ANDRZEJ SKORUPA<sup>\*)</sup>, JAAP SCHIJVE<sup>\*\*)</sup>,  
TOMASZ MACHNIEWICZ<sup>\*)</sup>, PAWEŁ KORBUT<sup>\*)</sup>

## FATIGUE CRACK GROWTH BEHAVIOUR OF 18G2A STEEL UNDER CONSTANT AMPLITUDE LOADING AND FOLLOWING A SINGLE OVERLOAD

Effects of specimen thickness and stress ratio on fatigue crack growth and crack closure levels under constant amplitude loading and after a single overload have been studied experimentally for a structural steel (18G2A). The corresponding crack growth data from the fatigue tests have been presented and evaluated. The experimental trends have been compared to those reported in the literature for various steels. The ability of the effective stress intensity factor range based on crack closure measurements to correlate the observed crack growth response has been investigated.

### Nomenclature

$a$	=	crack length
$a_{OL}$	=	crack length at application of the overload
CA	=	constant amplitude
CC	=	crack closure
$da/dN$	=	fatigue crack growth rate
DCPD	=	direct current potential drop
FCGR	=	fatigue crack growth rate
$K$	=	stress intensity factor
$K_{max}$ ( $K_{min}$ )	=	maximum (minimum) level of $K$ of a fatigue cycle
$K_{op}$	=	crack opening level of $K$

<sup>\*)</sup> *University of Mining & Metallurgy, Al. Mickiewicza 30, 30-059 Kraków, Poland; E-mail: mskorupa@uci.agh.edu.pl*

<sup>\*\*)</sup> *Delft University of Technology, Kluyverweg 1, P.O.Box 5058, 2600 GB Delft, The Netherlands; E-mail: schijve@lr.tudelft.nl*

---

$N$	=	number of cycles
$N_D', N_D''$	=	delay periods (alternative definitions)
OL	=	overload
$r_{OL}$	=	overload plastic zone size
$R$	=	stress ratio
$S$	=	applied stress
$S_{max} (S_{min})$	=	maximum (minimum) level of $S$ of a fatigue cycle
$S_{OL}$	=	overload stress level
$S_{op}$	=	crack opening level of $S$
$t$	=	specimen thickness
$\Delta a_{OL}$	=	overload-affected crack growth increment
$\Delta K$	=	stress intensity factor range ( $K_{max} - K_{min}$ )
$\Delta K_{eff}$	=	effective stress intensity factor range ( $K_{max} - K_{op}$ )
$\Delta S$	=	applied stress range ( $S_{max} - S_{min}$ )

## 1. Introduction

Understanding the behaviour of fatigue cracks is essential for safe operation of structures subjected to cyclic loads in service. A host of experimental studies have shown that the fatigue crack growth rate (FCGR) depends in a complex way on variables related to material, loading, specimen thickness and geometry, microstructure and environment. A salient feature of the crack growth behaviour under variable amplitude loading is its dependence on the previous load history. Such a phenomenon is referred to as load interaction effects.

Since Elber [1] discovered in the late sixties that fatigue cracks can open or close above the minimum load of a fatigue cycle, crack closure (CC) has been considered to play a significant role in fatigue crack growth. Specifically, CC is often cited as the mechanism responsible for the effects of stress ratio, e.g. [2], and specimen thickness, e.g. [3], on FCGRs. Also, CC is considered to be the major cause of load interaction effects, specifically the retarded crack growth following an overload (OL) cycle, as reviewed in [4].

This paper examines, firstly, the effects of specimen thickness ( $t$ ) and stress ratio ( $R$ ) on fatigue crack growth in a low carbon structural steel under constant amplitude (CA) loading and CA loading with an intermittent OL. The corresponding results of the fatigue crack growth tests are presented and evaluated. A comparison is made between the observed experimental trends and those reported in the literature for various steels. Next, a correlation is sought between the observed FCGRs and the CC behaviour measured throughout the fatigue tests. The work was intended to create an experimental data bank for structural steel required to improve a crack growth prediction model developed by the authors [5].

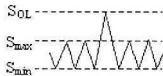
### 2. Experimental techniques

The material used is 18G2A low carbon structural steel, composition 0.14C-1.36Mn-0.21Si-0.020P-0.020S-0.11Cu-0.11Cr-0.05Ni. The microstructure in the rolling direction consists of alternate bands of ferrite and pearlite, the average diameter of ferrite grains being of 10 μm. Mechanical properties in the rolling direction are: yield stress = 392 to 402 MPa, tensile strength = 536 to 544 MPa, and elongation to failure = 22 to 28%. Central crack tension specimens of various thicknesses (Fig. 1a) were machined from a 20 mm thick plate with the specimen axis in the rolling direction. Prior to testing, all specimens were stress-relieved by slow heating in a furnace to 580°C and holding for 5 hrs, followed by a slow furnace cool. The central starter notch was made by electrical-discharge machining and its dimensions were in agreement with the ASTM Standard E 647-95a. Specimen surfaces were cleaned and polished to 1μm prior to testing to aid visual crack measurements.

All fatigue crack growth tests were performed under load control at 15 to 30 Hz. A survey of the experiments is given in Table 1. The  $R=0$  and  $R=0.5$  tests were run under the same applied stress range ( $\Delta S = S_{max} - S_{min}$ , Table 1) of

Tables 1.

Design of the fatigue crack growth tests



Specimen No.	Stress ratio R	Thickness t (mm)	Test type		Stress levels (MPa)		
			CA	OL	S <sub>min</sub>	S <sub>max</sub>	S <sub>OL</sub>
0205	0	4	✓		4.3	84.3	
0206	0.5	4	✓		80	160	
0211	0.7	4	✓		116.67	166.67	
0204	0	8	✓		4.3	84.3	
0202	0	12	✓		4.3	84.3	
0205	0.5	12	✓		80	160	
0212	0.7	12	✓		116.67	166.67	
0213	0	17	✓		4.3	84.3	
0210	0	4		✓	4.3	84.3	164.3
0209	0.5	4		✓	80	160	240
0208	0	12		✓	4.3	84.3	164.3
0207	0.5	12		✓	80	160	240
0214	0	17		✓	4.3	84.3	164.3

80 MPa. In the  $R = 0.7$  tests  $\Delta S = 50$  MPa was used to avoid a premature net-section yielding at the  $S_{\max}$  level. Fatigue precracking up to the half crack length ( $a$ ) of 10 mm was carried out at the same  $\Delta S$  level as that applied in the fatigue crack growth test. A single 100% OL, defined as  $(S_{OL} - S_{\min}) / (S_{\max} - S_{\min}) = 2$ , (see Table 1) was always applied at a frequency of 0.1 Hz at the half crack length  $a_{OL} = 13$  mm, namely when the fatigue crack advanced 3 mm after precracking had been completed. All tests were conducted in laboratory air using a Dartec computer-controlled closed-loop servohydraulic fatigue machine with load capacity of 250 kN.

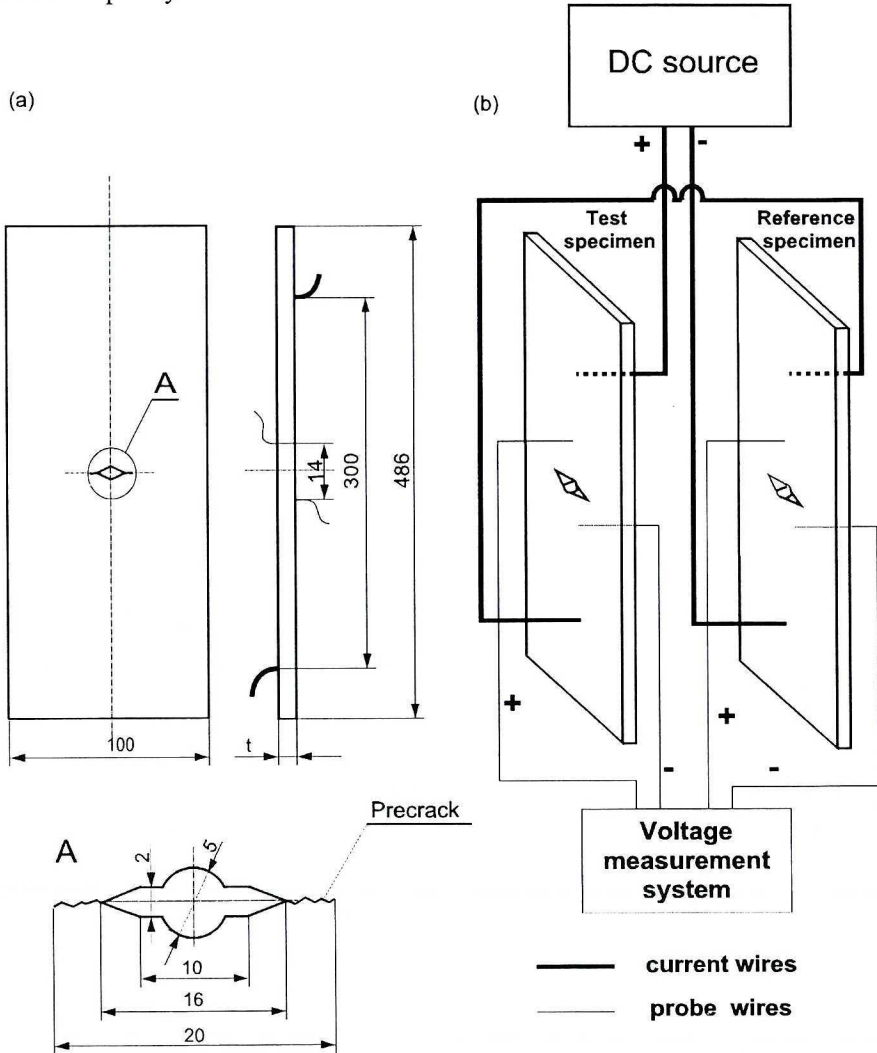


Fig. 1 Fatigue specimen geometry, dimensions in mm (a) and schematic of electrical connections for the DCPD measurements of crack length (b)

The crack length was monitored both by a direct current potential drop (DCPD) method and visually. The DCPD technique was used with a reference specimen, as recommended in ASTM Standard E 647-95a. The positions of the current leads and probe wires are shown in Fig. 1b. The machine was stopped at the  $S_{max}$  level for recording the DCPD signal. The visual observations of crack length incorporated an optical system consisting of a travelling microscope coupled with a video camera. A support system of the microscope with the screw mechanisms driven by the step engines provides facilities for its vertical and horizontal travel. The image of the crack tip region is displayed with a magnification of  $\times 150$  to  $300$  on a computer monitoring screen with adjustable vertical and horizontal scale lines. A computer program is used to control the displacements of the microscope along the specimen width and length directions and to determine the crack tip coordinates. The DCPD technique was applied to observe crack growth at crack length increments of below  $0.1$  mm. The visual crack length measurements were used to calibrate the DCPD method and to check if the ASTM Standard E 647-95a requirements on crack path deviations and on the crack symmetry with respect to the specimen vertical axis were met. In order to eliminate the effects of temperature fluctuations and of possible variations in specimen geometry on the accuracy of crack length measurements, an individual calibration of the DCPD signal was made for each specimen. The average of crack length readings taken by the travelling microscope at either side of the central notch was used with that purpose. Under stationary crack growth conditions, the visual crack length records were made at crack growth increments ranging from  $0.5$  to  $2.5$  mm at the lowest and highest FCGRs, respectively. The crack growth transient behaviour following an OL was monitored visually at crack length intervals below  $0.2$  mm.

The so called local compliance technique [6] was applied to periodically monitor the CC behaviour on the specimen surface throughout some of the fatigue tests. The mechanical compliance methods of CC measurements, including the technique used here, capture the CC behaviour by detecting compliance changes associated with opening and closing the fatigue crack. A set of 5 to 7 strain gauges of  $0.6$  mm in length and  $1$  mm in width were previously bonded on a specimen at the location approximately  $0.5$  mm above and below the expected crack path. A signal from the quarter bridge gauges was phase-matched to the load feedback signal sampled. Then, the signal was filtered by a 2-pole Butterworth lowpass filter and converted into a digital signal of a 19-bit resolution and  $10$  kHz sampling rate. Load versus strain records were taken simultaneously from several gauges at various locations behind and ahead of the crack tip. The load versus strain data have been evaluated to obtain the inflection point using a numerical procedure based on the slope deviation [7]. The highest inflection point in the load versus strain curve was usually found from a gauge located at a smallest distance behind the crack tip and this point was assumed to indicate the crack opening level. Typically, the CC behaviour was measured at the points where the centre line of the strain gauge was located,

0.8 to 1.5 mm behind the current crack tip. Attempts to monitor the bulk closure response over the whole crack front of thicker specimens proved to be unsuccessful. Neither an "Elber" clip gauge of 6 mm gauge length mounted straddling the fatigue crack along the specimen centre line nor a strain gauge of 6 mm in length bonded on the specimen side surface gave any indication of CC.

Observations on the fatigue fracture surfaces were made macroscopically and microscopically. The macroscopic examination occurred with the unaided eye and with a small magnifying glass (8x). The microscopic fractography was carried out in a scanning electron microscope (SEM). Samples were cut from the fatigue specimens including the area between the spark eroded notch and the final fracture of the specimen. The fracture surfaces were cleaned and gold sputtered. The samples were then mounted in the SEM (Jeol JSM-840 A) equipped with a SEMafore, a digital image recording system. It was tried, both macroscopically and microscopically, to see the crack front marking of the OL and to reveal possible striations.

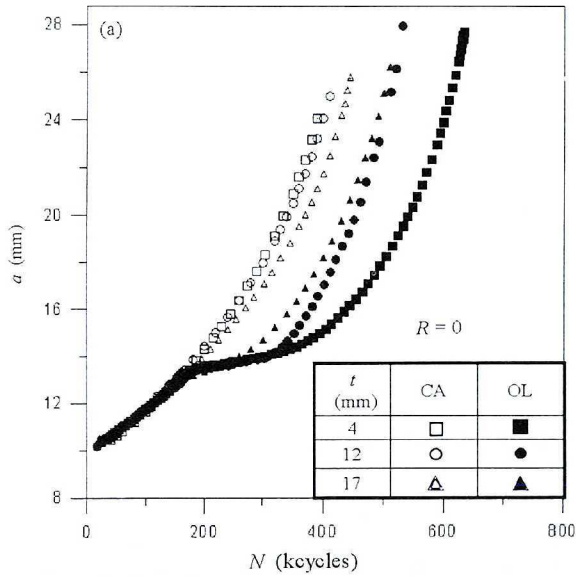
### 3. Fatigue crack growth tests

#### 3.1. Results

The crack growth curves from all tests, except for Specimen 0204 for which the results are nearly identical as those for Specimen 0205, are plotted in Figs 2a and b where  $N$  denotes number of cycles after precracking. Data points for which net-section yielding occurred at the  $S_{\max}$  level have been cropped. The OL cycles introduced crack growth retardation in all tests and the retardation effect at a given  $R$ -ratio decreased as specimen thickness was increased. Under CA loading conditions, however, the influence of  $t$  was negligible.

The FCGRs ( $da/dN$ ) were computed from the data presented in Fig. 2. An incremental polynomial method using a 7-point fit was employed to smooth the  $a$  vs.  $N$  records, according to ASTM Standard E 647-95a. The results are shown in Figs 3 and 4 by plotting  $da/dN$  as a function of the stress intensity factor range ( $\Delta K$ ). Here,  $\Delta K = K_{\max} - K_{\min}$ , where  $K_{\max}$  and  $K_{\min}$  denote the maximum and minimum level respectively of the stress intensity factor in a loading cycle. The figures confirm the trend already evident from Fig. 2 that no systematic influence of specimen thickness on FCGRs in the CA test results is observed. Figs 4a and b illustrate that at  $R=0.5$  the specimens of 4 mm and 12 mm thickness show higher FCGRs than at  $R=0$ . For specimen thickness of 12 mm the  $da/dN$  vs.  $\Delta K$  data for to  $R=0.5$  and  $0.7$  fall along a single line (Fig. 4b) whereas the FCGRs for the 4 mm thick specimens are higher at  $R=0.7$  than at  $R=0.5$  (Fig. 4a).

(a)



(b)

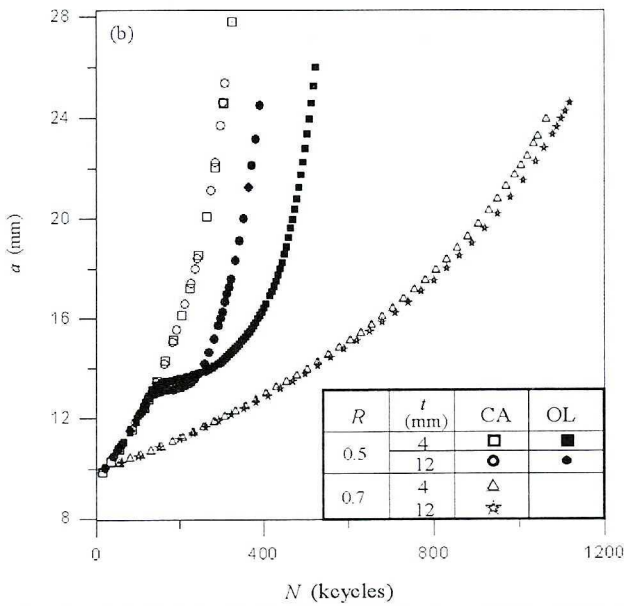


Fig. 2 Crack growth curves from all fatigue tests: (a) at  $R = 0$ ; (b) at  $R = 0.5$  and  $0.7$

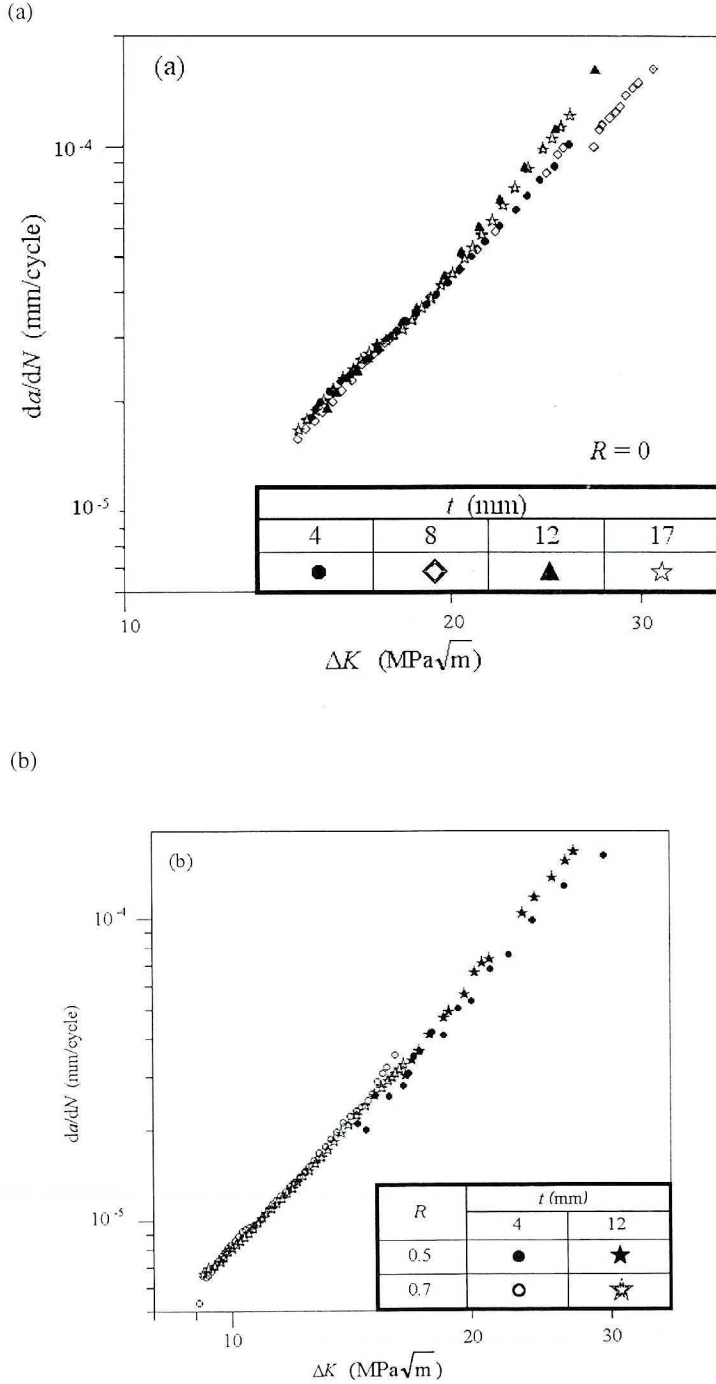
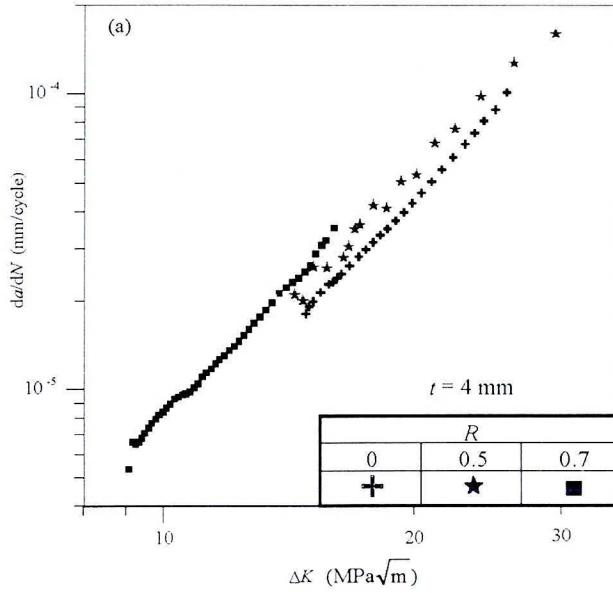


Fig. 3 The effect of specimen thickness on crack growth rates under CA loading at various stress ratios: (a) at  $R = 0$ ; (b) at  $R = 0.5$  and  $0.7$

(a)



(b)

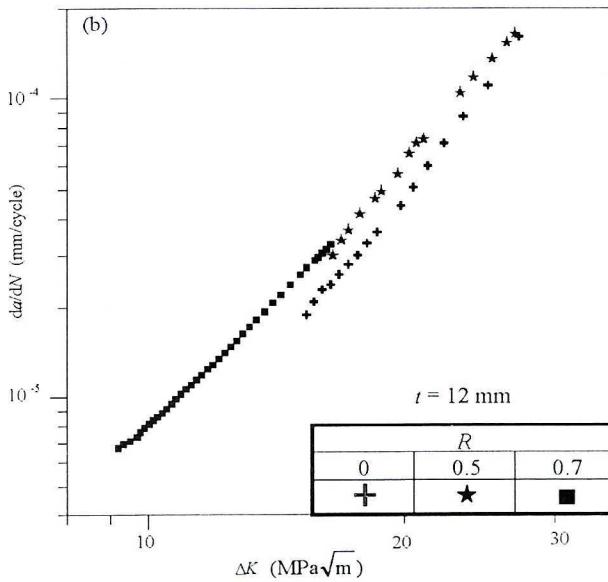


Fig. 4 The effect of stress ratio on crack growth rates under CA loading: (a) in 4 mm thick specimens; (b) in 12 mm thick specimens

Figs 5 and 6 highlight the influence of the test variables on post-OL transients of the FCGR. As seen in Figs 5a and b, a thinner specimen always shows more retardation than a thicker specimen at the same  $R$ -ratio. This trend is more pronounced when specimen thicknesses of 4 mm and 12 mm are considered whereas only minor differences can be noted between the behaviour of the 12 mm thick and 17 mm thick specimens. The thickness effect is more significant at  $R=0.5$  (Fig. 5b) than at  $R=0$  (Fig. 5a). Note in Fig. 5a that in the case of the 4 mm thick specimen  $da/dN$  never actually reaches the stationary value pertinent to CA crack growth whilst for the thicker specimens the retardation phase is followed by accelerated crack growth.

It is apparent in Fig. 6a that the retarded FCGRs observed in the  $R=0$  and  $R=0.5$  test on the 4 mm thick specimens coincide, except at highest  $\Delta K$ . This behaviour is in contrast to that shown in Fig. 6b by the 12 mm thick specimens. Here the FCGRs recover slower from the minimum  $da/dN$  value at  $R=0$  than at  $R=0.5$ .

The magnitude of the instantaneous load interaction effect after an OL can be represented by the FCGR observed in the OL tests,  $(da/dN)_{OL}$ , normalized by the FCGR measured in the CA tests at the same crack length for the same specimen thickness and  $R$ -ratio,  $(da/dN)_{CA}$ . It can be seen in Fig. 7 where the  $(da/dN)_{OL}/(da/dN)_{CA}$  ratios from all the tests are plotted against the post-OL crack increment  $(a - a_{OL})$  that the initial acceleration following an OL application only occurred in the  $R=0$  tests on the 4 mm thick and 12 mm thick specimen. This is also evident in Figs 5a and 6 where the  $da/dN$  values measured in the above mentioned two tests jump immediately after the OL above the level observed in the corresponding CA tests. Fig. 7 further shows that the minimum in FCGRs is always attained when the crack has grown some distance after an OL. This implies that the so called delayed retardation occurred under all test conditions. The  $a - a_{OL}$  crack growth increment corresponding to the minimum post-OL  $da/dN$  value was nearly the same in all tests (0.38 - 0.51 mm), as also was the minimum  $(da/dN)_{OL}/(da/dN)_{CA}$  ratio (0.08 - 0.12 except of a higher value of 0.33 for the 17 mm thick specimen). From Fig. 7, for specimen thickness of 4 mm, more retardation occurred at  $R=0.5$  than at  $R=0$ . A conspicuous feature observed in Fig. 7 for the larger thicknesses and also apparent in Figs 5 and 6 is accelerated crack growth following the retardation phase. This effect is most pronounced for the 17 mm thick specimen.

The overall retardation effect induced by an OL can be quantified using the measures shown in Fig. 8, namely the delay period (defined alternatively as  $N_D'$  or  $N_D''$ ) and the delay distance also referred to as the OL-affected zone ( $\Delta a_{OL}$ ). Here  $\Delta a_{OL}$  is the crack growth increment after the OL necessary for the FCGR to return to the steady state value observed under CA loading and  $N_D''$  is the number of cycles required to grow the crack to this distance. Without the OL  $\Delta a_{OL}$  is grown in  $N_{CA}$  cycles which implies  $N_D' = N_D'' - N_{CA}$ , see Fig. 8. The

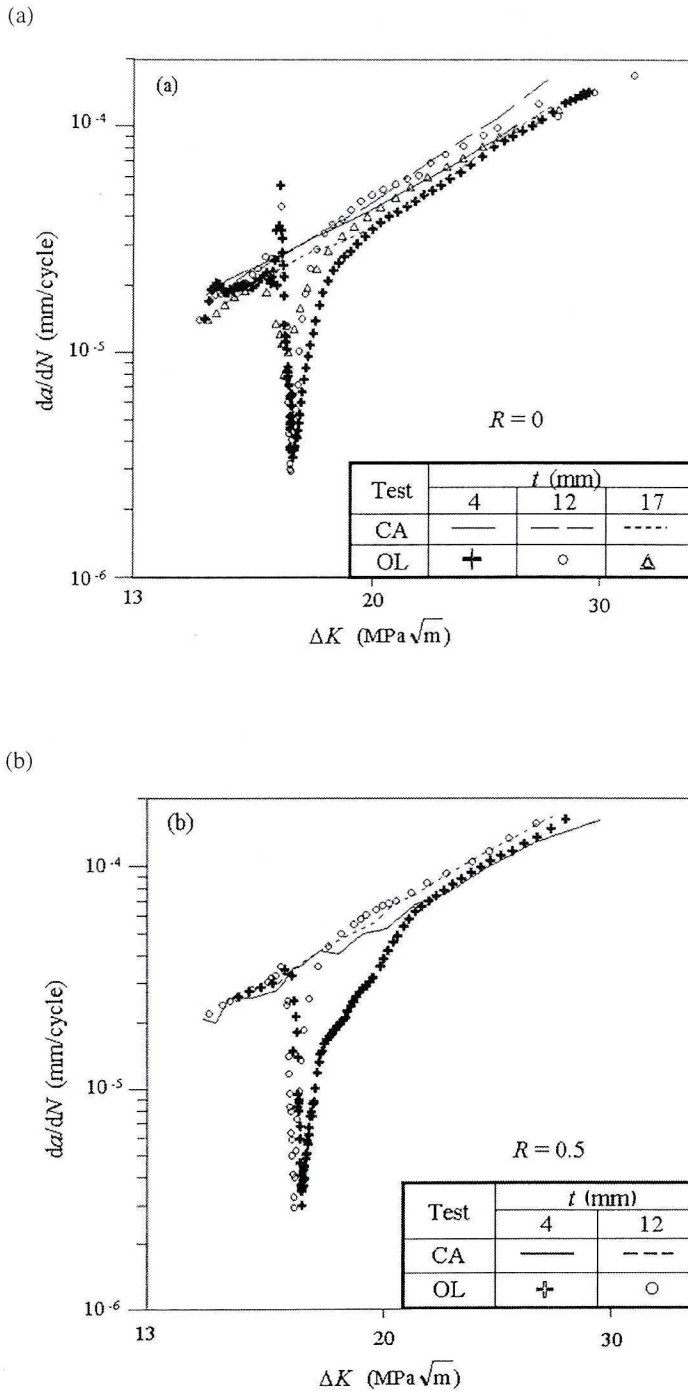
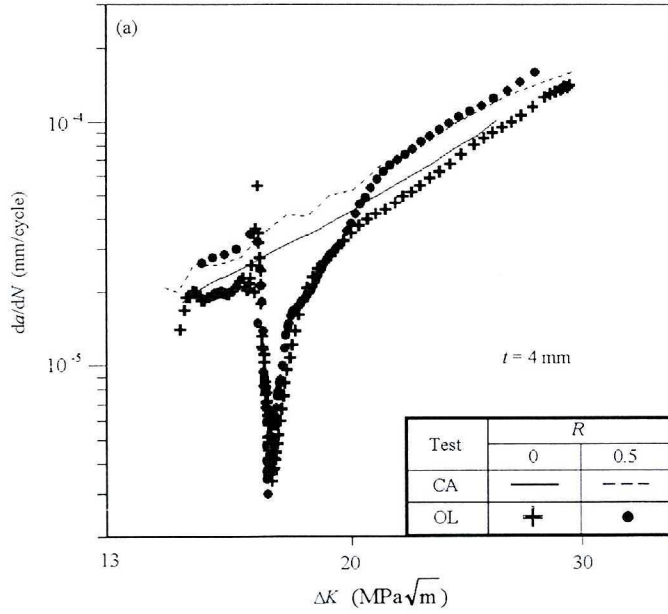


Fig. 5 The effect of specimen thickness on post-OL crack growth rates: (a) at  $R = 0$ ; (b) at  $R = 0.5$

(a)



(b)

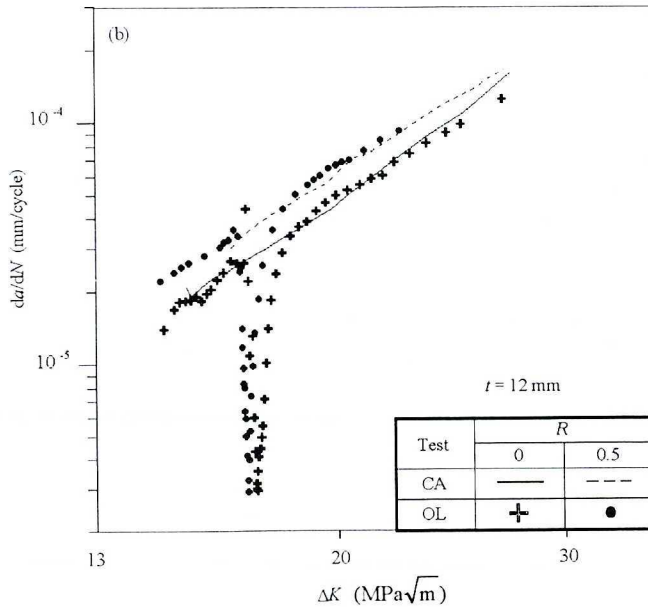


Fig. 6 The effect of stress ratio on post-OL crack growth rates: (a) in 4 mm thick specimens; (b) in 12 mm thick specimens

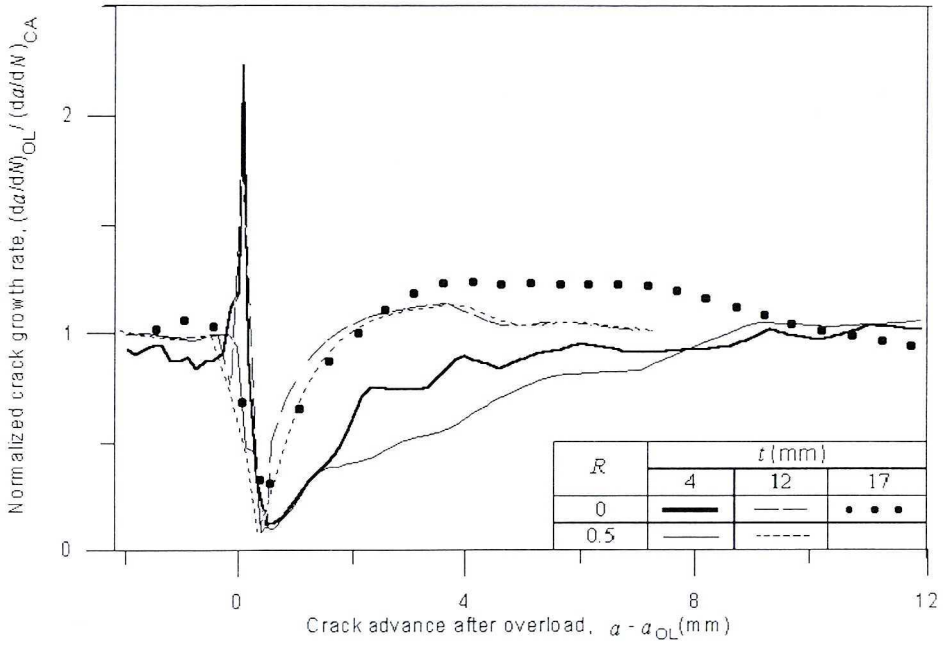


Fig. 7 Variations of normalized crack growth rates throughout the OL tests

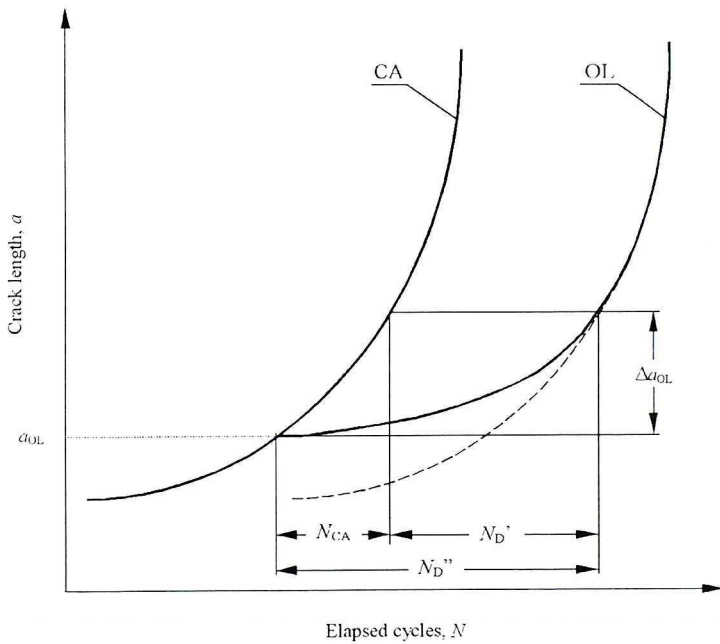


Fig. 8 Definition of parameters to quantify the retardation effect

normalized  $N_D''/N_{CA}$  parameter seems to be a more realistic measure of the amount of retardation than  $N_D'$  or  $N_D''$  as it quantifies the benefit from applying an OL under specific test conditions.

The observed effects of  $t$  and  $R$  on the retardation parameters depicted in Fig. 8 are summarized in Figs 9a and b. The  $N_D'$  vs.  $t$  data in Fig. 9a confirm the trend also visible in Fig. 2: increasing specimen thickness reduces the delay period. When the test results are viewed in terms of  $N_D''/N_{CA}$  vs.  $t$  it is apparent that larger profits from the OL application have been gained at  $R = 0.5$  than at  $R = 0$ . At  $R = 0$  the OLs brought about equally beneficial results for the 4 mm thick and the 12 mm thick specimen (same  $N_D''/N_{CA}$  values), whilst for the 17 mm thick specimen the OL effect on crack growth was dramatically smaller.

In terms of  $\Delta a_{OL}$ , the most effective was an OL applied on the 4 mm thick specimen in the  $R = 0$  test, Fig. 9b. The  $\Delta a_{OL}$  vs.  $t$  data further show that delay distances observed at  $R = 0$  for 12 mm and 17 mm specimen thickness are similar. A normalized parameter often cited in the literature, e.g. [8], [9], [10], is  $\Delta a_{OL}/r_{OL}$ , where  $r_{OL}$  is the OL plastic zone size. The  $\Delta a_{OL}/r_{OL}$  vs.  $t$  data with  $r_{OL}$  computed for plane stress conditions show similar tendencies as the  $\Delta a_{OL}$  vs.  $t$  data, Fig. 9b. Note that at  $R = 0$  the delay distances exceed the corresponding plastic zone sizes, i.e.  $\Delta a_{OL}/r_{OL} > 1$ , even for the thicker specimens.

### 3.2. Discussion

Some of the experimental trends reported here have also been observed in other works. Constant  $\Delta K$  tests on compact-tension (CT) specimens of carbon-manganese structural steels conducted by Fleck [3] at three different positive  $R$ -ratios and by Shuter and Geary [10] at  $R = 0$  revealed negligible differences in FCGRs for a range of specimen thicknesses, consistent with the present results (compare Fig. 3). However, in CA tests by Matsuoka and Tanaka on HT80 Q&T steel [11], FCGRs for an 18 mm thick central crack tension specimen exceeded those measured for a 2 mm thick specimen by a factor of over 2. It could be concluded based on the above-cited results that crack growth under CA loading conditions is more influenced by sheet thickness in higher strength steels than in lower strength steels.

Results reported in the literature demonstrate that the effect of  $R$ -ratio on crack growth under CA loading, especially in the Paris regime, is much less pronounced for steels than for Al alloys, compare e.g. [12] and [13]. In the present CA tests, the average ratio of the FCGRs at  $R = 0.7$  to those observed at  $R = 0$  at the same  $\Delta K$  level is about 1.5 which is within the range of the corresponding values reported for similar structural steels, e.g. [3], [12].

Crack growth transients following the application of a single OL during base line cycles of a smaller amplitude have been extensively studied on a variety of materials, see a review work [14]. Results generated on structural steels show that an increase of specimen thickness reduces the retardation phenomenon,

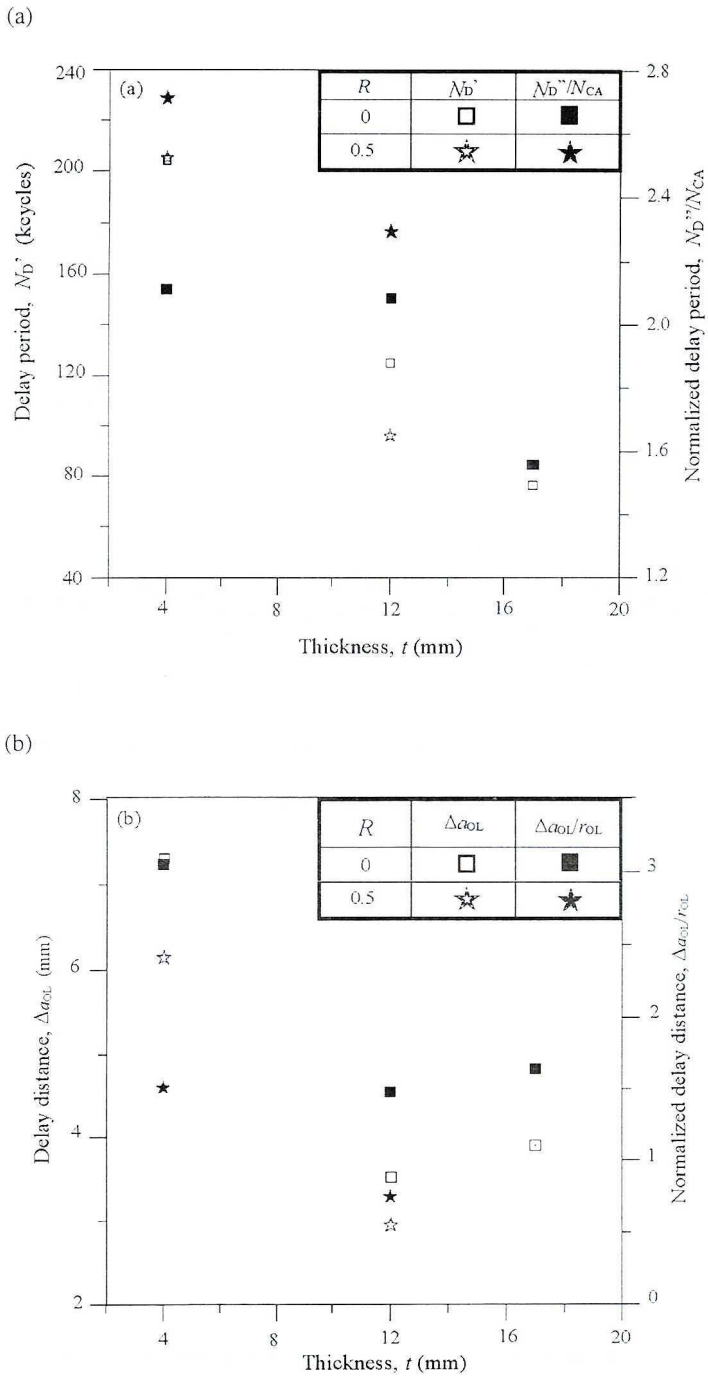


Fig. 9 The effects of specimen thickness and stress ratio on: (a) delay period; (b) OL-affected zone

both in terms of the delay period and the OL-affected zone [8], [10], [11], [15], which is in agreement with the present work (see Fig. 9). In tests on a high strength steel [15], the above trend was found to vanish when thickness exceeded a certain specific limit. The latter feature seems to be mirrored in our results only by the  $\Delta a_{OL}$  vs.  $t$  behaviour, Fig. 9b, whilst  $N_D'$  decreases linearly with increasing  $t$  values, Fig. 9a. It is noteworthy that Shuter and Geary [10] in  $K$ -controlled tests on a structural steel similar to the steel used here, obtained a linear relationship between  $\log N_D''$  and  $t$ . It implies a more significant effect of thickness on the delay period than found in the present tests. As recognized in many experimental studies including those on structural steels,  $\Delta a_{OL}$  measured on the surface of thinner specimens under base line loading at  $R=0$  can significantly exceed the OL-induced plastic zone size computed for plane stress conditions, whereas  $\Delta a_{OL}$  measured on the surface of thick specimens is always smaller than  $r_{OL}$  [8], [9], [15]. As pointed out earlier, in the present tests  $\Delta a_{OL}$  at  $R=0$  was in all cases greater than  $r_{OL}$  (Fig. 9b).

Further differences between the present results and those reported in other works are revealed through a more detailed insight into retardation transients. In the works referred to above, Fleck [8] and Shuter and Geary [10] observed that an increase of specimen thickness caused the minimum in  $da/dN$  to occur earlier and become less deep. In contrast, Figs 5 and 7 demonstrate that both the minimum  $da/dN$  value and the distance at which this minimum is reached do not depend on thickness. It is apparent that specimen thickness affects retardation only in the stage when FCGRs are recovering from the minimum value.

Systematic investigations on  $R$ -ratio effects on post-OL crack growth transients in structural steels are lacking in the literature. Direct comparisons between our results and those reported for a structural steel by Shuter and Geary [10] cannot be made because at an  $R$ -ratio of 0.1 and 0.5 these workers applied an OL level which equalled twice the base line  $K_{max}$ . In  $K$ -controlled tests on 6 mm thick CT specimens in stainless steel, Shin and Hsu [9] noted the normalized minimum FCGR to become higher and  $\Delta a_{OL}$  to decrease as the  $R$ -ratio was increased. Only the latter trend is in accordance with the present results for specimen thickness of both 4 and 12 mm, Fig. 9b.

A distinct feature of the present results is that maximum retardation occurred more immediately after an OL than reported for steels elsewhere [8], [9], [10], [16]. The ratio of the minimum  $da/dN$  position from the point of OL to the OL-affected zone size ranges in our tests from 0.05 to 0.15 which is much lower than most values estimated from test data presented in the above-mentioned works.

In contrast to the present work, all literature results cited here have been obtained from  $K$ -controlled tests. Hence, it cannot be excluded that the differences between the post-OL crack growth behaviour observed here and that reported by others may stem not only from material related aspects but also from the different loading conditions and type of specimen.

## 4. Crack closure behaviour

### 4.1. Measurement results

Under CA loading conditions CC results were only obtained for the  $R=0$  tests because at the two higher  $R$ -ratios (0.5 and 0.7) closure was not detected. Although no CC was indicated in the  $R=0.5$  tests before the OL was applied, closure was observed to develop after the OL. Under CA loading the mean values of the crack opening stress ( $S_{op}$ ) measured for the 4 mm thick and 17 mm thick specimen were 28 and 27 MPa respectively. The insignificant differences between the CA closure responses for both specimen thicknesses are in accordance with the negligible thickness effect on crack growth behaviour revealed under CA loading (compare Figs 2 and 3).

Exemplary results on the measured  $S_{op}$  variations throughout a CA and OL test are shown in Fig. 10 for specimen thickness of 4 mm and  $R=0$  loading. It is evident that the post-OL closure transients in Fig. 10 directly correspond to the crack growth transients shown in Fig. 5a. The initial drop of  $S_{op}$  below the pre-OL value reflects the brief initial acceleration of crack growth. The subsequent decelerated growth rates are mirrored by the progressive increase of  $S_{op}$  to a level higher than that prior to the OL. The subsequent gradual decrease of  $S_{op}$  to a value below that of the base line loading corresponds to approaching the stationary FCGR levels pertinent to CA loading.

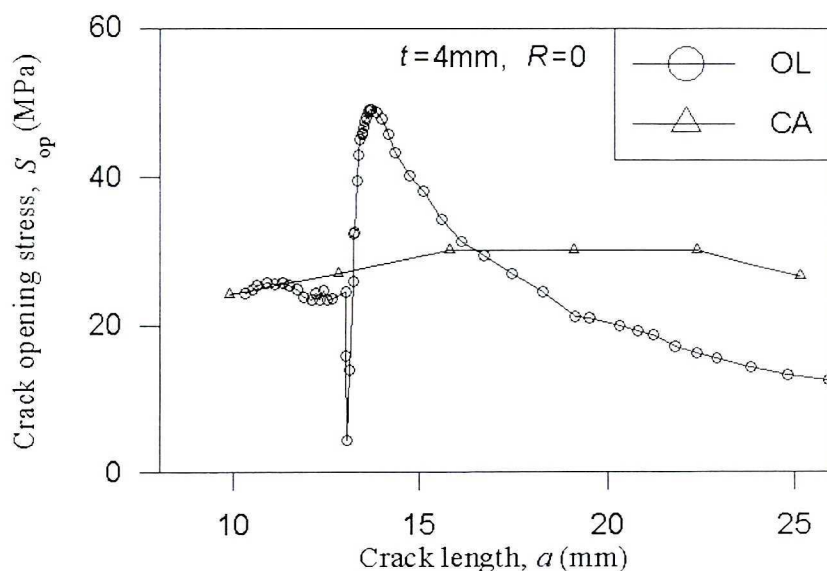


Fig. 10 Crack opening stresses measured by the compliance method for 4 mm thick specimen under CA loading and in the OL test at  $R=0$

The ability of CC to account for post-OL crack growth transients at  $R=0$  is further checked in Figs 11a and b by comparing predicted from CC behaviour and observed FCGRs for the 4 mm thick and 17 mm thick specimen respectively. The CC concept implies that the FCGR in a given cycle is controlled by the current level of  $\Delta K_{\text{eff}}$  and that the  $da/dN$  vs.  $\Delta K_{\text{eff}}$  relationship is the same for both CA and variable amplitude fatigue crack growth. Here,  $\Delta K_{\text{eff}}$  is the effective stress intensity factor range defined as  $K_{\text{max}} - K_{\text{op}}$ , where the crack opening stress intensity factor ( $K_{\text{op}}$ ) corresponds to the  $S_{\text{op}}$  stress level. For either specimen thickness, the master crack growth equation,  $da/dN=f(\Delta K_{\text{eff}})$ , was derived as the regression line for the  $da/dN$  vs.  $\Delta K_{\text{eff}}$  data from the CA test at  $R=0$ . The  $\Delta K_{\text{eff}}$  values were obtained from the measured  $S_{\text{op}}$  levels. The  $da/dN=f(\Delta K_{\text{eff}})$  equation with  $\Delta K_{\text{eff}}$  based on the measured CC response was then employed to predict the FCGRs for the OL tests. As seen in Fig. 11, the FCGR transients are qualitatively predicted except that the initial post-OL acceleration shown by the predicted FCGRs for the 17 mm thick specimen is not revealed by the observed results. Quantitatively, the observed and predicted data correlate well for the 4 mm thick specimen (Fig. 11a). Unfortunately, the predictions could not be made for the regime of maximum retardation because the corresponding low  $da/dN$  values were not observed in the CA  $R = 0$  test. Consequently, the  $da/dN=f(\Delta K_{\text{eff}})$  master relationship based on the latter test did not validate the growth rates  $da/dN < 10^{-6}$  mm/cycle. The quantitative agreement between the observed and predicted FCGRs for the 17 mm thick specimen (Fig. 11b) is less satisfactory than in the case of the 4 mm thick specimen, especially in the period when the FCGRs are increasing from the slowest transient value to the stationary crack growth.

The  $\Delta K_{\text{eff}}$  values calculated on the basis of the crack opening levels measured in all experiments are presented against the corresponding observed  $da/dN$  values in Fig. 12. Additionally, the  $R=0.7$  test results are plotted also. Because no closure was detected under the  $R=0.7$  loading, it was assumed that in this case  $\Delta K = \Delta K_{\text{eff}}$ . As seen in Fig. 12, the closure concept can fully account for the OL effect for the specimen thicknesses and the stress ratios considered. However, the data at  $R=0.7$  are considerably separate from the other data, as would be also the results of the  $R=0.5$  CA test (not shown in the figure for the sake of clarity) in which CC also was not detected. Probably, the results in Fig. 12 should lead to the conclusion that CC is not the only reason for the  $R$ -ratio effect on crack growth.

## 4.2 Discussion

A prominent role of plasticity-induced CC in causing delayed retardation following an OL has been suggested by both direct and indirect experimental evidence outlined in a review paper [4]. Reported comparisons between closure results obtained using various mechanical compliance techniques demonstrate

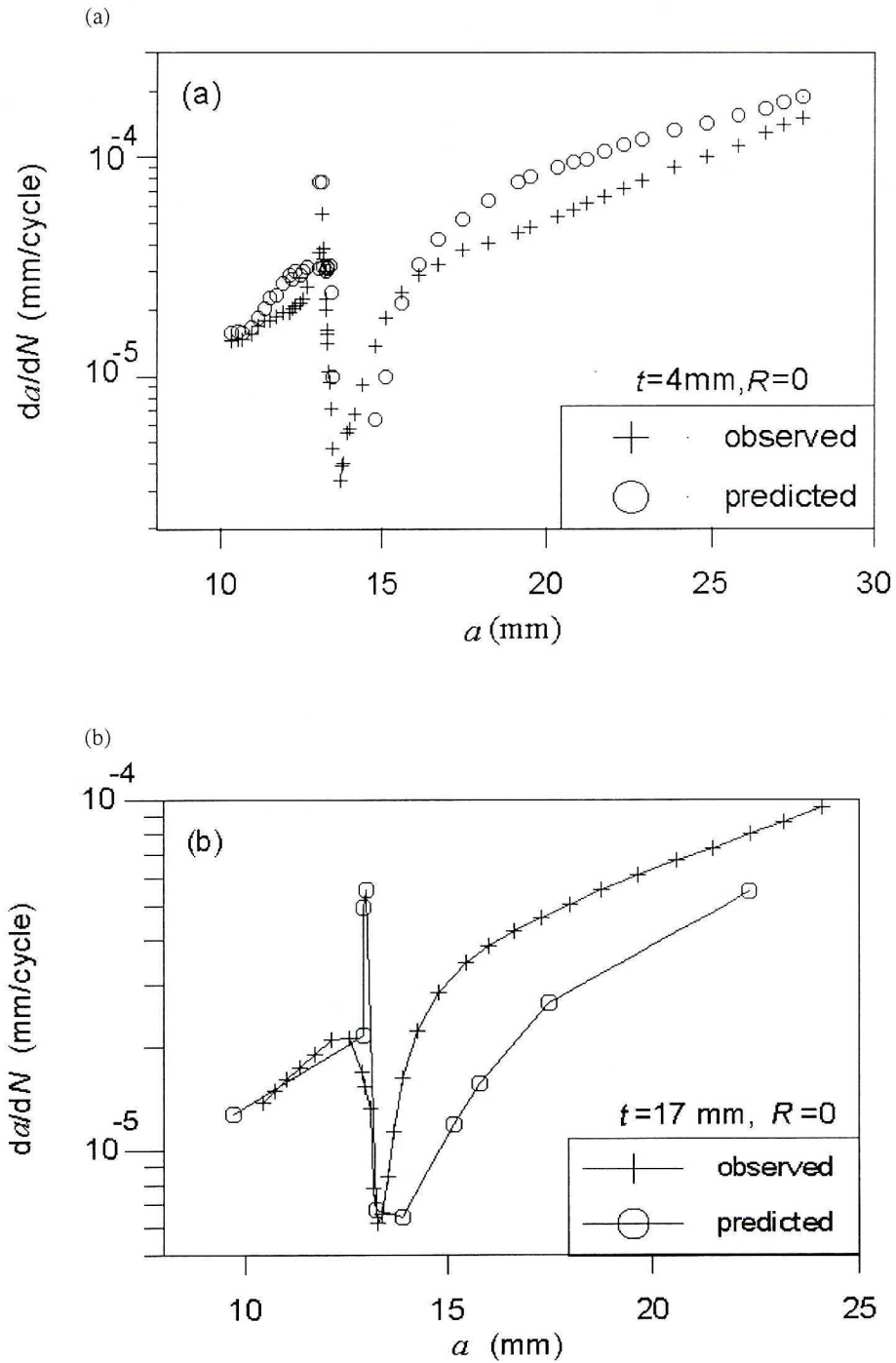


Fig. 11 Comparison of predicted (from closure measurements) and observed post-OL transient crack growth responses at  $R = 0$ : (a) for 4 mm thick specimen; (b) for 17 mm thick specimen

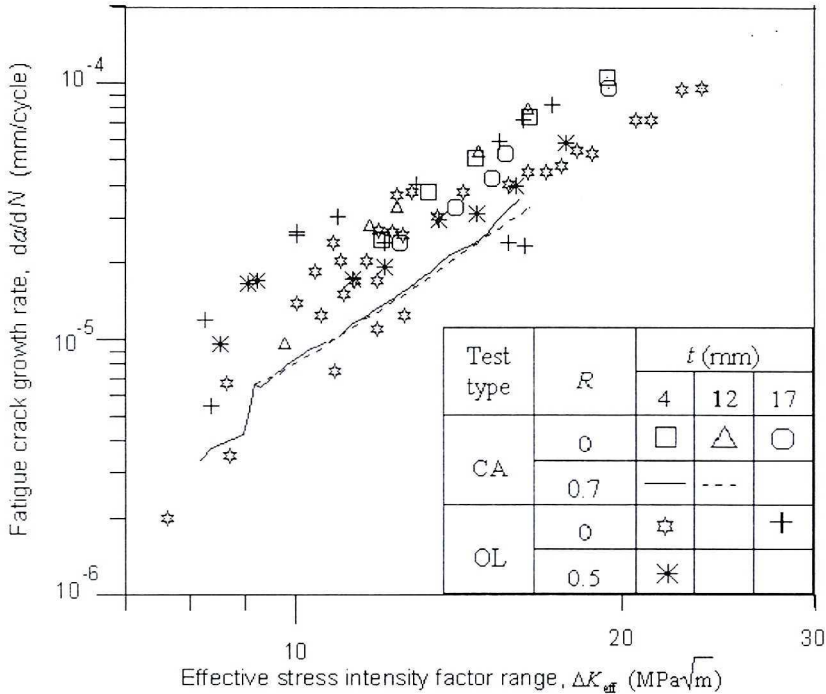


Fig. 12 Relationship between the observed fatigue crack growth rates and the effective stress intensity factor range based on crack closure measurements

beyond any doubt that only the local (i.e. near crack tip) measurements, as performed in this investigation, are able to capture subtle features of the CC transient behaviour following a single OL, e.g. [17].

Several authors, e.g. [8], [9], [16], [17], compared observed post-OL FCGRs in steel specimens and those predicted from the measured CC response using the procedure described in Section 4.1. Typically, FCGRs measured and inferred from CC show a better agreement until the minimum  $da/dN$  value is attained than beyond this point when the predicted values tend to be lower than the observed results. The same trends are shown by the data in Fig. 11b and - to some extent - also in Fig. 11a. Such a behaviour is sometimes attributed to the phenomenon of discontinuous closure [8], [9], [16]. As first suggested by Fleck [8], in the period when FCGRs are recovering from the minimum value, the crack flanks are open near the crack tip, but still touch at the crack tip position of the OL. As a result, compliance measurements indicate artificially high closure levels corresponding to the first contact between the „humps” produced by the OL rather than to the first contact just behind the crack tip. The occurrence of discontinuous closure has been corroborated by crack profile

measurements at lower stress ratios [8], [9], [16]. However, based on numerical analysis results, Tsukuda et al. [18] refute this phenomenon except at  $R \geq 0.5$ . Ward-Close and Ritchie [19] totally negate the occurrence of discontinuous closure referring to their observations that primary surface contacts during post-OL transients are always immediately adjacent to the crack tip. In the context of the controversies about discontinuous closure, the reasons for the systematic discrepancies between observed and predicted from CC post-OL FCGRs remain obscure.

The influence of specimen thickness on the amount of retardation is among trends that can be rationalized using plasticity-induced CC arguments. An OL will generate a larger plastic zone under plain stress conditions at the crack tip than in the plane strain state. Hence, a more operative closure mechanism and, thereby, more retardation can be expected for thinner specimens because plane stress conditions are more easily reached. The data in Fig. 12 indicate that thickness effects observed in the present tests are handled properly by applying the measured closure results, as also reported by Fleck for structural steel [3], [8].

Results on the ability of the  $\Delta K_{\text{eff}}$  parameter based on CC measurements to account for the effect of  $R$ -ratio on crack growth are miscellaneous. Results demonstrating a good consolidation of the  $da/dN$  vs.  $\Delta K_{\text{eff}}$  data corresponding to various  $R$ -ratios, e.g. [3], and results still indicating that the  $R$ -ratio effects on crack growth do not wholly disappear in the  $da/dN$  vs.  $\Delta K_{\text{eff}}$  plot, e.g. [12], can both be found in the literature. Finite element method analyses by Tsukuda et al. [12] indicated that plasticity-induced CC occurred in a medium carbon structural steel under CA loading for  $R$ -ratios up to 0.7. As  $R$  was increasing, the distance behind the crack tip over which the crack was closed at minimum load, was noted to decrease from 0.4 mm at  $R = 0$  to 0.016 mm at  $R = 0.7$ . However, these authors failed to detect CC by using the local compliance technique in their crack growth tests conducted at  $R \geq 0.5$ . Similarly, no CC was detected in other works, including the present study, for the Paris region of crack growth in tests on various type steels conducted under  $R \geq 0.5$  CA loading conditions [3], [9], [10]. Tsukuda et al. [12] have suggested that changes in compliance related to the CC phenomenon for high  $R$ -ratio loadings are too small to be visualized in the load-displacement diagram even if high sensitivity measurement instrumentation is used. Hence, a conclusion that the CC concept cannot sufficiently account for the influence of  $R$ -ratio on crack growth can be erroneous.

More work seems to be required to recognize which of the two possible reasons, namely inaccuracies in CC measurements or an inability of the  $\Delta K_{\text{eff}}$  parameter to correlate with the crack growth behaviour, should account for differences between the observed crack growth behaviour and the corresponding CC response.

## 5. Fractography

The macroscopic examination of the fatigue fracture surfaces indicated that each OL cycle produced a marking line which was vaguely visible only. It was slightly curved, i.e. the crack length at mid thickness was larger than at the specimen surface, a difference in the order of 0.5 mm. Curved crack fronts corresponding to OL cycles were also reported by Matsuoka and Tanaka [11]. Shear lips, typically observed for aluminium alloys [20] and also for a high strength steel [11], were not formed.

An OL marking line observed in the SEM was rather tortuous, and at a high magnification could not always be followed continuously over the full thickness of the specimen, Fig. 13. Close to the specimen surface, the OL marker lines could not be observed any more. A tentative explanation is that these lines may have been erased due to enhanced closure in the „plane stress” regions near the specimen surfaces.

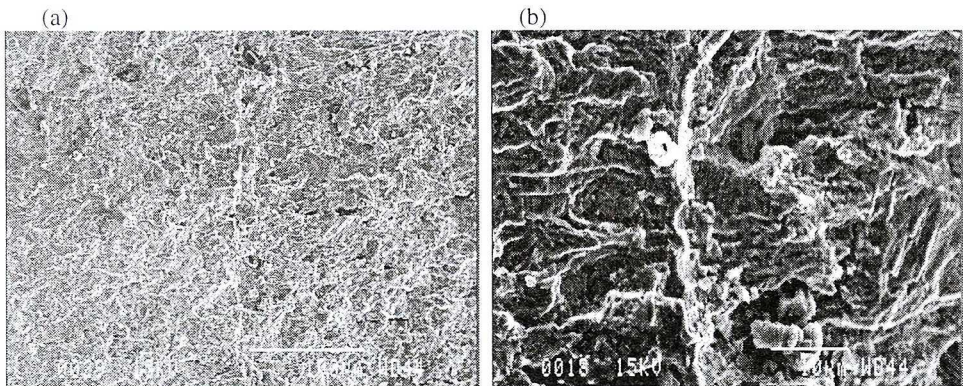


Fig. 13 SEM micrographs of the fracture surface of Specimen 0207 at the OL position: (a) at a lower and (b) at a higher magnification. Vertically, in the centre of both pictures the crack front of the OL

The fatigue fracture surfaces showed a rather irregular pattern with tortuous lines, as also evident for a low carbon steel (0.18C, 0.92Mn) from a SEM examination by Shuter and Geary [10]. Their micrographs revealed striations caused by blocks of 500 OL cycles, with the striation spacing in agreement with the FCGR (in the order of 1  $\mu\text{m}/\text{cycle}$ ) corresponding to these OL cycles. In the present study, however, no evidence of striations of the base line fatigue load cycles was found in the SEM. Apparently, the corresponding FCGR (in the range of 0.01 – 0.1  $\mu\text{m}/\text{cycle}$ ) was too low to lead to an easy detection in the SEM for this type of steel. In this respect, fatigue fracture surfaces of cracks in Al-alloys can be more instructive because they usually show many striations. Also, the correlation between a variable amplitude load history and the striation pattern has been found to be most useful [21].

## 6. Conclusions

Effects of specimen thickness and stress ratio on fatigue crack growth and closure behaviour in a structural steel (18G2A) have been investigated experimentally under constant amplitude loading and after a single overload. The following conclusions have been reached:

1. For constant amplitude loading, a negligible influence of specimen thickness on fatigue crack growth and a slight increase of crack growth rates with increasing a stress ratio were observed. These trends are consistent with results reported in the literature for structural steels.
2. The transient crack growth response following an overload depends on the specific combination of specimen thickness ( $t$ ) and stress ratio ( $R$ ). At an  $R$  of 0 and 0.5, the delay period decreases with increasing specimen thickness. In terms of the normalized delay period, the benefit from an overload at  $R = 0.5$  is larger than at  $R = 0$ . The effects of  $t$  and  $R$  on crack growth retardation predominantly occur during the period when the crack growth rate is recovering from the minimum value, while these effects are negligible prior to this minimum (i.e. in the delayed retardation period). Differences between the experimental trends found in the present tests and those reported in the literature may stem from material and specimen geometry related aspects as well as from differences in the loading conditions.
3. The measured post-overload crack closure response is in qualitative agreement with the observed crack growth behaviour. However, differences similar as those noted by other authors are revealed between the empirical crack growth rates and the predicted growth rates based on the measured closure levels.
4. The results demonstrate that the measured closure behaviour does account for the observed influence of specimen thickness and for the post-overload transients, but it cannot fully account for the effects of stress ratio. Further investigation is required to determine underlying reasons behind the disparities between the crack growth behaviour and the measured closure response.
5. Fractography of the fatigue fracture surfaces indicated slightly curved marker lines of the overload cycles. Striations of the base line cycles could not be observed, also because crack growth rate was too low for such observations. The fracture surfaces made a rather tortuous impression.

## 7. Acknowledgements

The authors would like to acknowledge the partial financial support of the State Committee for Scientific Research via Grant No. PB 1459/T07/97/12.

Manuscript received by Editorial Board, December 27, 1999;  
final version, April 15, 2000.

#### REFERENCES

- [1] Elber W.: Fatigue crack closure under cyclic tension. *Engng Fracture Mech.*, 1970, Vol. 2, pp. 37+45.
- [2] Tanaka K.: Mechanics and micromechanics of fatigue crack propagation. *ASTM STP 1020*, 1989, pp. 151+183.
- [3] Fleck N.A.: An investigation of fatigue crack closure. Cambridge University Engineering Dept. report CUED/C-MATS/TR.104, May 1984.
- [4] Skorupa M.: Load interaction effects during fatigue crack growth under variable amplitude loading - a literature review. Part II: qualitative interpretation. *Fatigue Fract. Engng Mater. Struct.*, 1999, Vol. 22, pp. 905+926.
- [5] Skorupa M., Schijve J., Skorupa A. and Machniewicz T.: Fatigue crack growth in structural steel under single and multiple periodic overloads. *Fatigue Fract. Engng Mater. Struct.*, 1999, Vol. 22, pp. 879+887.
- [6] Skorupa A. and Skorupa M.: Crack closure measurement techniques. *Mechanika*, Kwartalnik AGH, 1998, Vol. 17, z. 4, pp. 577+592 (in Polish).
- [7] Philips E.P.: Results of the second round robin on opening-load measurement conducted by ASTM Task Group E24.04.04 on crack closure measurement and analysis. National Aeronautics and Space Administration, Hampton, Virginia, November 1993.
- [8] Fleck N.A.: Influence of stress state on crack growth retardation. *ASTM STP 924*, 1988, Vol. 1, pp. 157+183.
- [9] Shin C.S. and Hsu S.H.: On the mechanisms and behaviour of overload retardation in AISI 304 stainless steel. *Int. J. Fatigue*, 1993, Vol. 15, pp. 181+192.
- [10] Shuter D.M. and Geary W.: Some aspects of fatigue crack growth retardation behaviour following tensile overloads in a structural steel. *Fatigue Fract. Engng Mater. Struct.*, 1996, Vol. 19, pp. 185+189.
- [11] Matsuoka S. and Tanaka K.: The influence of sheet thickness on delayed retardation phenomena in fatigue crack growth in HT80 steel and A5083 aluminium alloy. *Engng Fracture Mech.*, 1980, Vol. 13, pp. 293+306.
- [12] Tsukuda H., Ogiyama H. and Shiraishi T.: Fatigue crack growth and closure at high stress ratios. *Fatigue Fract. Engng Mater. Struct.*, 1995, Vol. 18, pp. 503+514
- [13] Zhang S., Marissen R., Schulte K., Trautmann K.K., Nowack H. and Schijve J.: Crack propagation studies on Al 7475 on the basis of constant amplitude and selective variable amplitude loading histories. *Fatigue Fract. Engng Mater. Struct.*, 1987, Vol. 10, pp. 315+332.
- [14] Skorupa M.: Load interaction effects during fatigue crack growth under variable amplitude loading - a literature review. Part I: empirical trends. *Fatigue Fract. Engng Mater. Struct.*, 1998, Vol. 21, pp. 987+1006.
- [15] Tokaji K., Ando Z., Nagae K. and Imai T.: Effect of sheet thickness on fatigue crack growth retardation and validity of crack closure concept. *Fatigue 84*, Proc. 2nd Int. Conf. Fatigue

- and Fatigue Thresholds, 3-7 September 1984, University of Birmingham, UK, Edited by C.J. Beevers, Chameleon Press, pp. 727÷737.
- [16] Shercliff H.R. and Fleck N.A.: Effect of specimen geometry on fatigue crack growth in plane strain-II. Overload response. *Fatigue Fract. Engng Mater. Struct.*, 1990, Vol. 13, pp. 297÷310.
- [17] Dougherty J.D., Srivatsan T.S. and Padovan J.: Fatigue crack propagation and closure behaviour of modified 1070 steel: experimental results. *Engng Fracture Mech.*, 1997, Vol. 56, pp. 167÷187.
- [18] Tsukuda H., Ogiyama H. and Shiraishi T.: Transient fatigue crack growth behaviour following single overloads at high stress ratios. *Fatigue Fract. Engng Mater. Struct.*, 1996, Vol. 19, pp. 879÷891.
- [19] Ward-Close C.M. and Ritchie R.O.: On the role of crack closure mechanisms in influencing fatigue crack growth following tensile overloads in a titanium alloy: near threshold versus higher  $\Delta K$  behaviour. *ASTM STP 982*, pp. 93÷111.
- [20] Schijve J.: Shear lips on fatigue fractures in aluminium sheet material. *Engng Fracture Mech.*, Vol. 14, 1981, pp. 789÷800.
- [21] Schijve J.: The significance of fractography for investigations of fatigue crack growth under variable-amplitude loading. *Fatigue Fract. Engng Mater. Struct.*, 1999, Vol. 22, pp. 87÷99.

### **Wzrost pęknięć zmęczeniowych w stali 18G2A przy obciążeniach stałoamplitudowych i po pojedynczych przeciążeniach**

#### **Streszczenie**

Przedstawiono wyniki badań eksperymentalnych nad wpływem grubości próbki i współczynnika asymetrii cyklu na wzrost pęknięć zmęczeniowych oraz poziom zamykania się pęknięcia w stali 18G2A przy obciążeniach stałoamplitudowych i po pojedynczych przeciążeniach. Znalezione trendy eksperymentalne porównano z opublikowanymi wynikami innych prac otrzymanymi dla różnych stali. Zbadano możliwość korelacji prędkości wzrostu pęknięć ze wszystkich eksperymentów przy pomocy efektywnego współczynnika intensywności naprężeń opartego na wynikach pomiarów zamykania się pęknięcia.